Control of Boundary Layer Separation in Supersonic Flow Using Injection Through Microramps

S. Vaisakh and T.M. Muruganandam

Introduction

The separation of boundary layer is one of the most unwanted phenomena in high-speed aerodynamics [1]. This causes unwanted waves and pressure losses along with blockage of intake decreasing the intake efficiency. A common active control method to suppress separation is to remove the low momentum fluid near the wall, by bleed holes, which requires great amount of energy [2]. Passive flow control methods include cavity, vortex generators, microporous plate, mesoflaps, micro-vortex generators (MVGs), etc. [3–5]. Among these, MVGs are more popular in recent years. MVGs introduce streamwise vortices into the flow that energizes some parts of the low momentum fluid close to the wall, while having very low stagnation pressure losses. Detailed reviews on MVGs and their effect on performance enhancement by Lin [6] and Lu et al. [7] suggest that existence of low momentum region downstream of the MVGs makes them inefficient in separation control. Quantitative measurements [8–10] showed the ability of microramps to control shock-induced separation and flow features. Others [11–13] conducted a detailed analysis of the wake downstream of the microramps. Giepman et al. [14] concluded that the conventional MVGs are not adequate to eliminate the shock-induced separation, and they just caused a spanwise modulation of separation bubble.

There are other MVGs like "r vane" [15], ramped vane [16], tandem method [17], and slotted ramp [18] used in the literature that are partially effective, or they are applicable in narrow regions. Another variant is the use of air-jet vortex generators [19], where the counter-rotating vortices generated by injection strengthened the boundary layer, yet the separation bubble is not fully suppressed. Even after 50 years of research toward eliminating separation by using various less intrusive methods, none of these are able to replace the conventional bleed system. There have also been studies combining MVG and air-jet vortex generator [20, 21]. This paper demonstrates experimentally a new flow control device consisting of an array of MVGs with air injection (along the wall) through them. These MVGs were placed ahead of a normal shock which interacts with the boundary layer. Results obtained were compared with the results of a "baseline case" (no control device) and a conventional MVG case.

Experimental Facility

A blowdown-type wind tunnel is used in this study. A schematic of the wind tunnel test section is shown in Fig. 1. Stagnation temperature of the wind tunnel is at 302 K (±3 K). Mach number upstream of the normal shock is 1.48, and Reynolds number is 2.24×10^7 m^{-1}. After the nozzle, a constant area portion is provided to increase the boundary layer thickness so that the vortex generator height is less than the boundary layer thickness. Three different cases were studied as described below. Case A, which is the "baseline case," had no MVGs. In case B, conventional [22] MVGs are present in the upstream of normal shock. Three forward-facing microramps with a ramp height of 1 mm are installed on the tunnel floor. The ratio of ramp height to the boundary layer thickness is 0.3. Case C is a modified version of case B in which air is injected through the trailing edge of the microramp. The bottom block is replaced to change cases. Figure 1 also shows the MVG arrangement in the bottom block for case C. In both cases, the ramps are placed 70 mm from the leading edge of the bottom block.

MVG with injection had a tapering groove at the trailing edge of the ramp and a 2 mm diameter hole as shown. A chamber in the bottom block below the MVGs as shown

S. Vaisakh (✉) • T.M. Muruganandam
Department of Aerospace Engineering, Indian Institute of Technology Madras, Chennai, India
e-mail: vaisakh0123@gmail.com

G. Ben-Dor et al. (eds.), *30th International Symposium on Shock Waves 2*, DOI 10.1007/978-3-319-44866-4_68

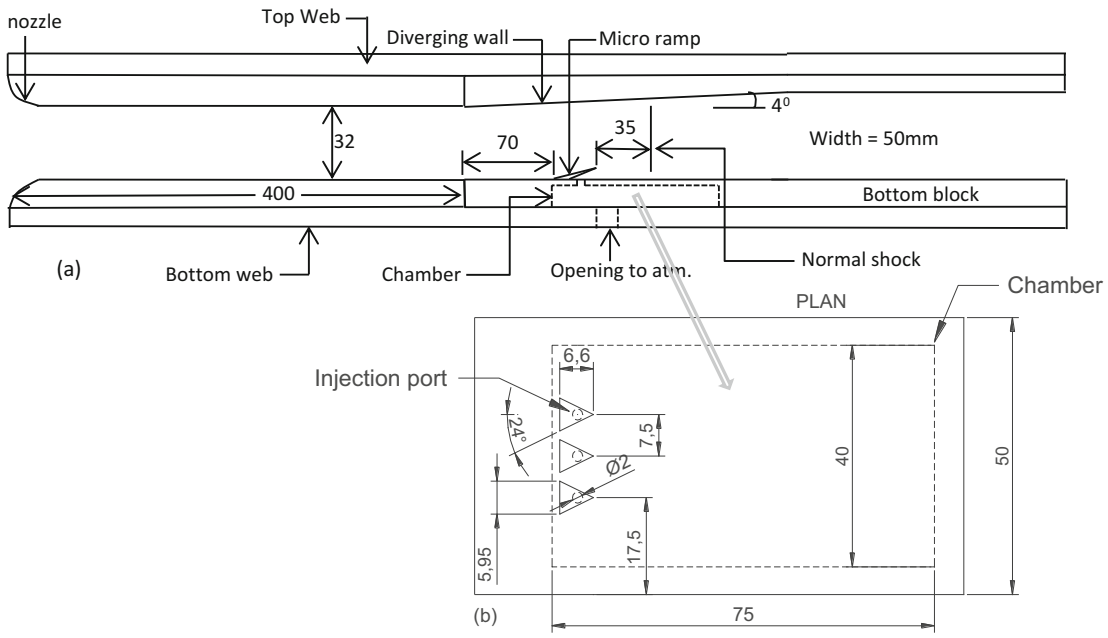

Fig. 1 Schematic of test setup. All dimensions in mm

in the figure supplies air for injection. When case C is operational, air from the atmosphere enters the chamber and is injected through the trailing edge of the ramp in the downstream direction. The pressure difference between chamber and trailing edge of ramp can cause choked injection.

Results and Discussions

Experiments were carried out for each of the cases described earlier, by maintaining the shock location at 112 mm from the start of the bottom block (35 h from trailing edge of MVGs, where h is the height of the microramp at trailing edge). This was achieved by adjusting the stagnation pressure. The normal shock is strong enough to separate the flow. Qualitative techniques such as schlieren and surface oil flow visualization are used to capture the shock wave/boundary layer interaction, along with wall pressure measurements. The following subsections present results from these individual techniques.

Figure 2 shows instantaneous (exposure 30 μs) schlieren images taken for all cases (A, B, and C) with horizontal knife edge coming from the bottom, so that the boundary layer appears as a bright layer at the bottom wall. There is a very weak oblique shock (WOS) coming from the tunnel floor whose effect is neglected. Case A shows the shock causing boundary layer separation in both the walls, having λ-foot. Case B shows that the MVG induces leading edge shock (LES) and trailing edge shock (TES) and an expansion region in between them. The wake behind the MVG rises higher than the MVG itself. Case C shows that when injection takes place through the trailing edge, TES is replaced with weak compression waves, and the MVG wake is thinner compared to that without injection. These indicate that, due to injection, there exists a higher momentum region downstream of the trailing edge. Therefore, a much fuller boundary layer exists downstream of this flow control configuration.

There exist low and high momentum regions in the wake of microramps [8, 14, 23]. The trailing edge shock is due to thickened boundary layer just downstream of the MVG [9] as seen from Fig. 2b. This thickened boundary layer containing low momentum regions are not capable of overcoming the adverse pressure gradients existing downstream of MVGs due to a shock [10, 11, 14]. This intermediate low momentum region makes the conventional microramps inadequate for complete separation control. From this, we can infer that the low momentum region present in the MVG wake is eliminated and this makes the injection through ramps more suitable for separation control.

Shock locations were captured from the sequence of images to track the shock movement in time. A sample of 600 frames (duration of 0.3 s) captured at the rate of 2000 fps is used for each case. The standard deviations obtained for cases A, B, and C are 1.50, 1.58, and 1.34 mm, respectively. The increased value of standard deviation for case B may be due to asymmetric separation. The lower value of standard deviation in case C implies that the shock is more stable. Later in this work, it can be correlated with lesser separation size. This stability in shock location is a welcome attribute in high speed intakes.

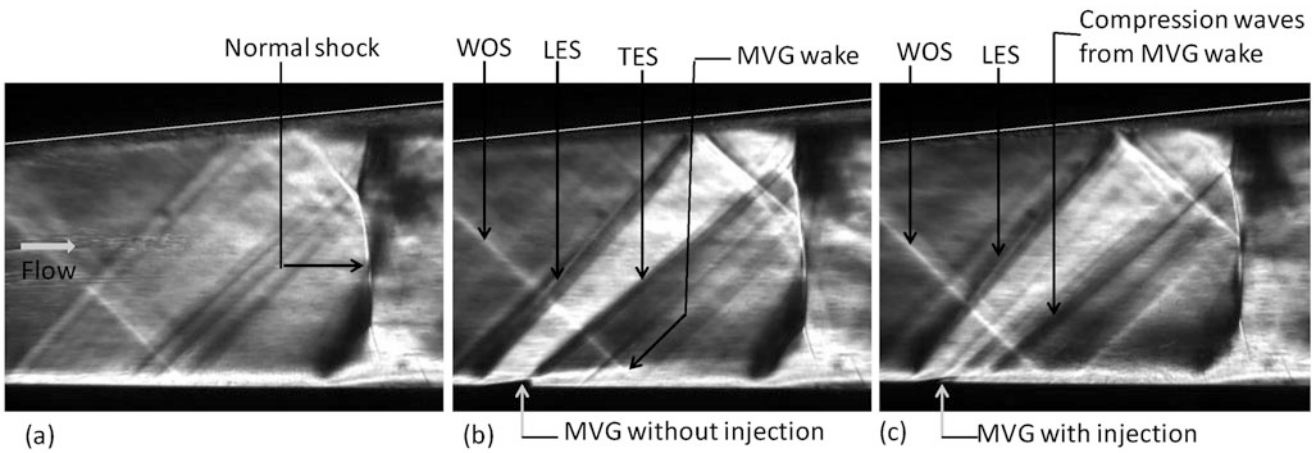

Fig. 2 Instantaneous schlieren images for (**a**) case A, (**b**) case B, and (**c**) case C. The shock location is maintained the same in all these cases

Oil flow visualization images are shown for the three cases in Fig. 3. The flow is from left to right. The shock location is marked by a vertical dotted line and the reattaching point is marked as "R" in the images. The shadow of the oil and tracer particle present in the corner region is falling on the tunnel floor for the illumination used. This shadow portion is pointed by letter "S" in Fig. 3. All the images are taken through the side wall glass window while the shock is at the required position, causing the images to be skewed. A sketch of the separation zones are also shown in the right side column of the figure for better perception. This is drawn based on manual observations of the slow-moving blobs of oil in the oil flow movies.

Figure 3a shows the surface flow visualization of the baseline case. There exists a large separation at the centerline region of the tunnel floor (dotted line region). There is a marginal upstream influence resulting from the corner separation indicated by a continuous white line. A small region of attached flow exists between centerline separation and corner separation. The centerline separation reattaches in the downstream of the flow while corner separation is growing continuously without any reattachment. In case B, the centerline separation length (L_{sep}) gets reduced. Moreover, the centerline separation becomes highly asymmetrical. Essentially, conventional MVGs are not strong enough to remove separation existing downstream of it, but they just rearrange the separation bubble, as was also observed by Giepman et al. [14]. The separation is more shifted toward one side of the tunnel floor. In general, the center separation widens in spanwise direction, reducing the width of intermediate attached flow between centerline and corner separation regions. The corner separation is also reduced compared to the baseline case, causing reduced upstream influence. However, there is a net reduction in separation length compared to baseline case.

In case C, the bulk centerline separation is replaced with a number of small separation pockets. L_{sep} decreases drastically, and there exists intermediate attached flow along the tunnel centerline. Flow pattern is more symmetrical compared to case B. The corner separation is more compared to cases A and B, and an increased upstream influence is witnessed. The coupling between corner effects and centerline separation is observed in literature already [24, 25] and is known that any decline in centerline separation can enhance corner separation and vice versa. In summary, this demonstrates that the MVGs with injection avoid separation and energize the flow near wall. While corner separation is increased slightly compared to the baseline case, this method is useful to avoid separation in high speed intakes. Additionally, this also decreases shock oscillations in the core flow.

Static wall pressure distribution (normalized by stagnation pressure) across the normal shock is shown in Fig. 4, for all three cases. The vertical line indicates the shock location. Case A shows increase in pressure ahead of the shock owing to the upstream influence. There is a steep increase in pressure near the shock, and the increase tapers off to achieve the final pressure farther downstream. In case B, the pressure does not increase until closer to the shock and then it increases steeply, and later tapers off to final pressure. In case C, the pressure rises earlier than case B, has similar pressure rise across shock, and reaches the final pressure the earliest.

When there is upstream influence, the corner separation occupies more volume and decreases space available for the flow, causing the supersonic flow to decelerate, thus increasing pressure. Downstream of the shock, the centerline

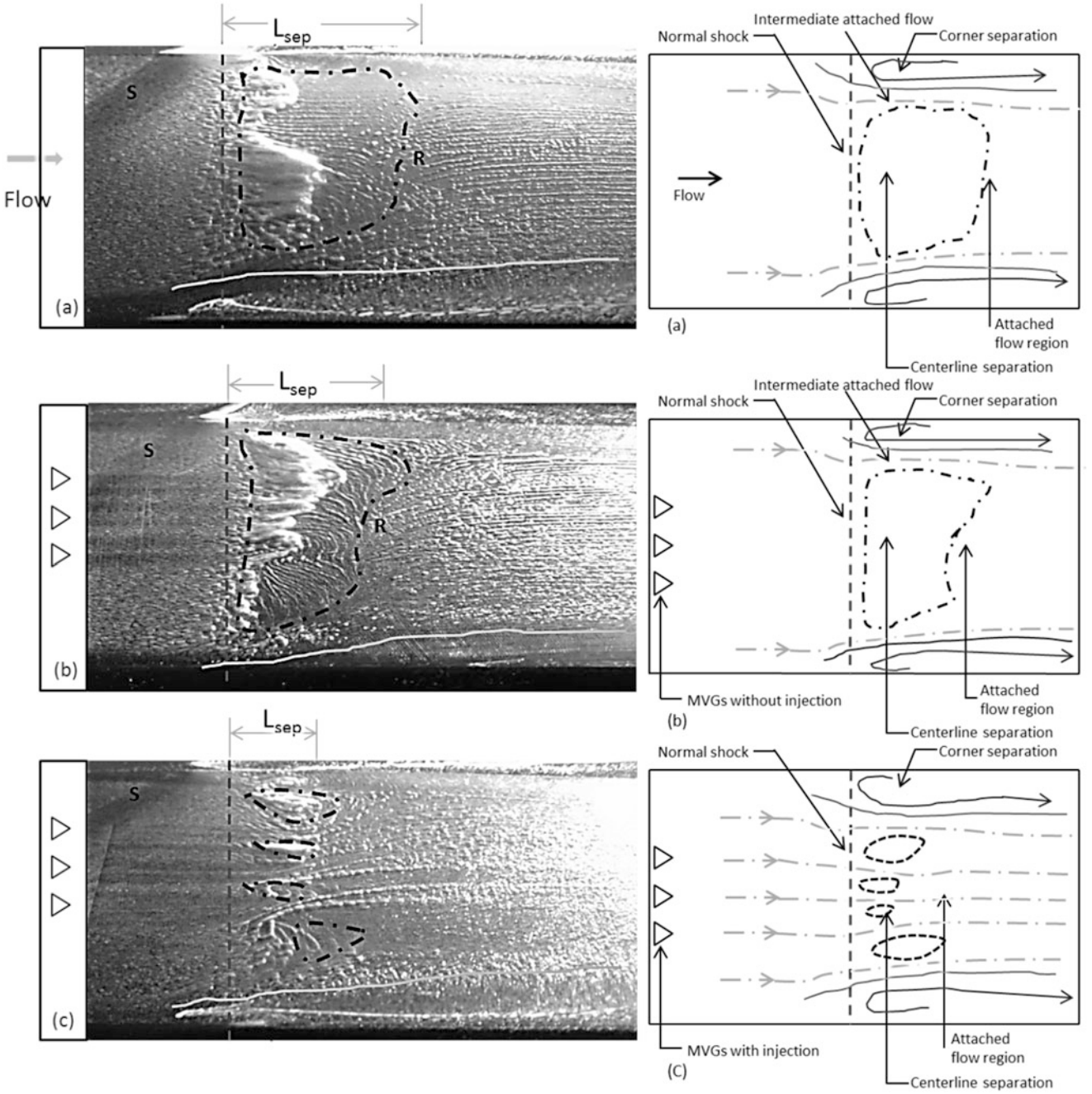

Fig. 3 Surface oil flow visualization for (**a**) case A, (**b**) case B, and (**c**) case C. A rough location of MVGs is also shown in the overlaid sketch. Also shown on the right side column are the schematic representations of the various separation zones in top view

separation causes the subsonic flow to accelerate delaying the pressure rise to the final value. In case B, the pressure curve is explained by the lower upstream influence, and a little decrease in centerline separation. Case C has higher upstream influence and very minimal centerline separation, explaining the pressure data. One can also note that case C is better in increasing the pressure across shock than the baseline case due to reduced centerline separation.

Conclusions

This study investigated efficacy of injection through MVGs to reduce separation behind a normal shock in a supersonic flow. Three cases, (A) baseline case—plain wall, (B) three numbers of conventional MVGs, and (C) same MVGs with injection of air through them, were investigated using

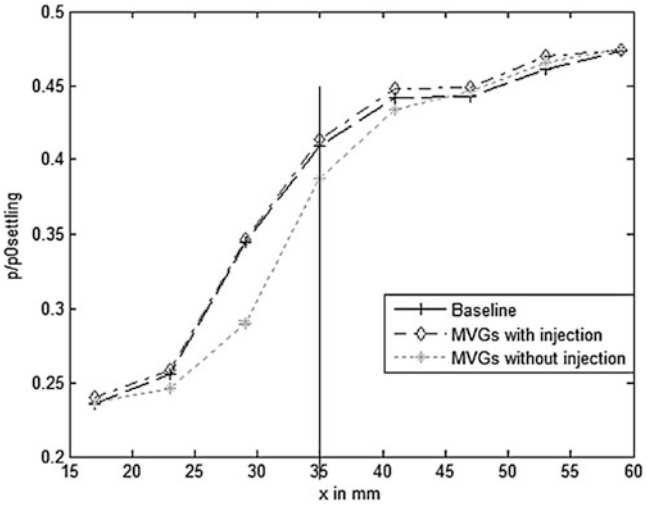

Fig. 4 Centerline wall pressure distribution for all the three cases. The distances are from the trailing edge of the ramps. Shock is at 35 mm from trailing edge of the MVGs

schlieren images, oil flow images, and wall pressure distribution.

Oil flow patterns show that, compared to case A, the conventional MVGs decreased both separation bubble and upstream influence through corner separation. Case C decreased the separation bubble to a large extent and also caused flow all along the tunnel floor in between the separation bubbles. Distributed wall jet injection through multiple MVGs causes a uniform increase of energy in the boundary layer across the span of the test section, suppressing separation to a large extent across the span. Schlieren images show that the case B has an oblique shock at the trailing edge and a growing low momentum region behind the MVGs. Case C, on the other hand, shows weak compression waves at the trailing edge of the MVGs and no growing low momentum regions. Case C had the most stable shock of all the three cases. Pressure data shows that the upstream influence due to the corner separation for case C is similar to case A, while the case B has lesser upstream influence. However, the pressure rise just downstream of shock is highest for case C due to the absence of large separation bubbles.

Injection through MVGs is an effective method to suppress boundary layer separation behind normal shocks and to decrease shock oscillations. While corner separation increases by a small amount, advantage to intake flows due to very small centerline separation is high.

References

1. Babinsky, H., Harvey, J.K.: Shock wave-boundary-layer interactions. Cambridge University Press, Cambridge, UK (2011)
2. Fukuda, M.K., Hingst, W.G., Reshotko, E.: Control of shock wave-boundary layer interactions by bleed in supersonic mixed compression inlets. NASA CR-2595. (1975)
3. McCormick, D.C.: Shock/boundary-layer interaction control with vortex generators and passive cavity. AIAA J. **31**(1), 91–96 (1993)
4. Srinivasan, K.R., Loth, E., Dutton, J.C.: Aerodynamics of recirculating flow control devices for normal shock/boundary-layer interactions. AIAA J. **44**(4), 751–763 (2006)
5. Ashill, P.R., Fulker, J.L., Hackett, K.C.: Research at DERA on sub boundary layer vortex generators (SBVGs), AIAA Paper 2001-0887, 39th AIAA Aerospace Science Meeting and Exhibit, Reno, NV, 8–11 January, (2001)
6. Lin, J.C.: Review of research on low-profile vortex generators to control boundary-layer separation. Prog. Aerospace Sci. **38**, 389–420 (2002)
7. Lu, F.K., Li, Q., Liu, C.: Microvortex generators in high-speed flow. Prog. Aerospace Sci. **53**, 30–45 (2012)
8. Babinsky, H., Li, Y., PittFord, C.W.: Microramp control of supersonic oblique shock-wave/boundary-layer interactions. AIAA J. **47** (3), 668–675 (2009)
9. Herges, T., Kroeker, E., Elliott, G., Dutton, J.C.: Microramp flow control of normal shock/boundary-layer interactions. AIAA J. **48** (11), (2010)
10. Blinde, P.L., Humble, R.A., VanOudheusden, B.W., Scarano, F.: Effects of micro-ramps on shockwave/turbulent boundary layer interaction. Shock Waves **19**, 507–520 (2009)
11. Bo, W., Weidong, L., Yuxin, Z., Xiaoqiang, F., Chao, W.: Experimental investigation of the micro-ramp based shock wave and turbulent boundary layer interaction control. Phys. Fluids **24**, 055110 (2012)
12. Sun, Z., Schrijer, F.F.J., Scarano, F., van Oudheusden, B.W.: Decay of the supersonic turbulent wakes from micro-ramps. Phys. Fluids **26**, 025115 (2014)
13. Wang, X., Yan, Y., Sun, Z., Liu, C.: The vortical structures in rear separation and wake produced by a supersonic micro-ramp. Flow Turb. Comb. **93**, 25–36 (2014)
14. Giepman, R.H.M., Schrijer, F.F.J., van Oudheusden, B.W.: Flow control of an oblique shock wave reflection with micro-ramp vortex generators: effects of location and size. Phys. Fluids **26**, 066101 (2014)
15. Titchener, N., Babinsky, H.: Microvortex generators applied to flow field containing a normal shock wave and diffuser. AIAA J. **49**(5), (2011)
16. Rybalko, M., Babinsky, H., Loth, E.: Vortex generators for a normal shock/boundary-layer interaction with a downstream diffuser. J. Prop. Power **28**(1), (2012)
17. Titchener, N., Babinsky, H.: Shock wave/boundary-layer interaction control using a combination of vortex generators and bleed. AIAA J. **51**(5), (2013)
18. Sharma, P., Ghosh, S.: A novel vortex generator for mitigation of shock-induced separation. 52nd Aerospace Sciences Meeting, (2014)

19. Souverein, L.J., Debie‘ve, J.F.: Effect of air jet vortex generators on a shock wave boundary layer interaction. Exp. Fluids **49**, 1053–1064 (2010)
20. Anderson, B.H., Mace, J.L., Mani, M.: Active “Fail Safe” micro-array flow control for advanced embedded propulsion systems. AIAA Paper 2009-741, (2009)
21. Gissen, A.N., Vukasinovic, B., Glezer, A.: Controlled streamwise vorticity in diffuser boundary layer using hybrid synthetic jet actuation. AIAA Paper 2009-4021, (2009)
22. Anderson, B., Tinapple, J., Surber, L.: Optimal control of shock wave turbulent boundary layer interactions using micro-array actuation. AIAA Fluids Engineering Conference, AIAA Paper 2006-3197, (2006)
23. Sun, Z., Scarano, F., van Oudheusden, B.W., Schrijer, F.F.J.: Numerical and experimental investigations of the supersonic microramp wake. AIAA J. **52**(7), (2014)
24. Bruce, P.J.K., Burton, D.M.F., Titchener, N.A., Babinsky, H.: Corner effect and separation in transonic channel flows. J. Fluid Mech. **679**, 247–262 (2011)
25. Burton, D.M.F., Babinsky, H.: Corner separation effects for normal shock wave/turbulent boundary layer interactions in rectangular channels. J. Fluid Mech. **707**, 287–306 (2012)